Mon. Not. R. Astron. Soc. **292,** 591–600 (1997)

On the topological stability of astrophysical jets

N. Vlahakis[1,2]★ and K. Tsinganos[1,2]★

[1]*Department of Physics, University of Crete, GR-710 03 Heraklion, Crete, Greece*
[2]*Foundation for Research and Technology Hellas (FORTH), GR-711 10 Heraklion, Crete, Greece*

Accepted 1997 July 11. Received 1997 May 22; in original form 1997 January 15

ABSTRACT

General theoretical arguments and various analytic self-similar solutions have recently shown that magnetized and rotating astrophysical outflows may become asymptotically cylindrical, in agreement with observations of cosmical jets. A notable common feature in all such self-consistent, self-similar MHD solutions is that before final cylindrical collimation is achieved, the jet passes from a stage of oscillations in its radius, Mach number and other physical parameters. It is shown that under rather general assumptions this oscillatory behaviour of collimated outflows is not restricted to the few specific models examined so far, but instead seems to be a rather general physical property of an MHD outflow that starts non-cylindrically before it reaches collimation. It is concluded thence that astrophysical jets are topologically stable to small-amplitude, time-independent perturbations in their asymptotically cylindrical shape. Also, similarly to the familiar fluid instabilities, these oscillations may give rise to brightness enhancements along jets.

Key words: instabilities – MHD – plasmas – stars: mass-loss – ISM: jets and outflows – galaxies: jets.

1 INTRODUCTION

Astrophysical jets have by now been widely observed in several cosmical environments, from the rich variety of stellar objects to active galactic nuclei (AGN) and quasars (e.g. see reviews by Biretta 1996, Ferrari et al. 1996 and Ray 1996). Three key aspects of the theoretical problem posed by the observations of jets are (i) the construction of self-consistent dynamical equilibria describing the initial acceleration and final collimation of the outflow; (ii) the examination of the stability properties of the beam and the detailed energetics of the outflow together with the *in situ* acceleration of particles and subsequent emission of radiation; and (iii) the modelling of the time-dependent problem.

Since magnetic fields seem to play a pivotal role in the acceleration, collimation and emission of radiation in jets, one may try to answer these questions by considering to lowest approximation the magnetohydrodynamic (MHD) description. For example, in meridionally self-similar models (Sauty & Tsinganos 1994, henceforth ST94; Trussoni, Sauty & Tsinganos 1996) the outflow is accelerated by a combination of gas pressure gradients and magnetocentrifugal forces; after the outflow crosses the (modified by self-similarity) slow/fast magneto-acoustic surfaces (Tsinganos et al. 1996), the jet is confined either magnetically or by the thermal gas pressure. Similar is the situation in radially self-similar (Blandford & Payne 1982; Fiege & Henriksen 1996) or translationally self-similar MHD models (Chan & Henriksen 1980; Bacciotti & Chiuderi 1992).

★E-mail: vlahakis@physics.uch.gr (NV); tsingan@physics.uch.gr (KT)

Regarding the question of classical stability of collimated outflows, it is well known that low Mach number, laboratory fluid beams maintain their directionality for relatively short distances, typically 10 times their diameter. The basic reason for beam disruption is the familiar Kelvin–Helmholtz (KH) instability due to the motion of the fluid of the beam relative to the surrounding medium (Ferrari, Trussoni & Zaninetti 1978, 1981; Ferrari et al. 1996). Linear KH stability analysis (Ferrari et al. 1978, 1981) predicts that the most unstable modes are of the order of the circumference of the beam times its Mach number, $\lambda_{KH} \sim 2\pi R_j M_j$, while typical times of the fastest growing modes are of the order of the ratio of the circumference of the beam to the sound or Alfvén speed times its Mach number, $\tau_{KH} \sim 2\pi(R_j/c_s)M_j$. Nevertheless, astrophysical jets, observed first in association with extragalactic radio sources and secondly in association with young stellar objects, often extend over distances which are a much larger multiple of their width. Apart from the occasional wiggles and knots of enhanced surface brightness along their length, these astrophysical jets appear to survive for much longer periods than the time-scales on which the linear analysis of the KH instability predicts that they should break up. In order to investigate possible saturation effects of the linear phase of the instability, the non-linear evolution of the KH hydrodynamic instability has also been followed (Bodo et al. 1994, 1995). In this case, it is found that the persistence of the jet depends principally on the density contrast with the ambient medium and the Mach number.

In addition to the KH instabilities, magnetized jets are also subject to current-driven instabilities which are well known to

create great difficulties in the confinement of laboratory plasmas. In superfast magnetosonic jets with speeds exceeding the fast MHD speed, the kinetic energy dominates the sum of the magnetic and thermal energies and therefore the KH instability growth rates are an order of magnitude or so higher than the growth rates of the kink instabilities (Appl & Camenzind 1992; Appl 1996). Instead, in *transfast* magnetosonic jets, the current and fluid instabilities have comparable effects.

Probably related to the stability of jets, a notable aspect of available self-consistent MHD equilibrium solutions is that the beam width and other parameters undergo small-amplitude oscillations which often decay with distance from the source (Chan & Henriksen 1980; Bacciotti & Chiuderi 1992; ST94; Contopoulos & Lovelace 1994). These exact and quasi-analytic solutions have been obtained under specific assumptions such as the corresponding self-similarity Ansatz. The aim of this paper is to investigate further the question that naturally arises then: whether the particular features of oscillations in the jet's width can be obtained from the general set of MHD equations, regardless of specific models. Hence, we shall examine the *topological* stability of an MHD outflow which is asymptotically collimated, and together with its ambient medium consists of a compressible plasma of infinite conductivity. Classical stability theory addresses the question of whether a given equilibrium configuration evolves away from (unstable) or back toward (stable) the initial state when perturbed. In the present context, topological stability refers to the question of whether a given equilibrium state preserves its topological properties when subjected to a perturbation. We should keep in mind that topologically stable configurations may well be unstable from the classical point of view. However, since, for sufficiently slow time variations, the outflow can be modelled by a sequence of quasi-static (equilibrium) states, the topological stability of a configuration may provide evidence on its classical stability.

2 PERTURBATIONS OF COLLIMATED OUTFLOWS

Consider the steady ($\partial/\partial t = 0$) hydromagnetic equations,

$$\rho(\boldsymbol{V}\cdot\nabla)\boldsymbol{V} = \frac{(\nabla\times\boldsymbol{B})\times\boldsymbol{B}}{4\pi} - \nabla P - \rho\nabla\mathcal{V}, \tag{1}$$

$$\nabla\cdot\boldsymbol{B} = 0, \quad \nabla\cdot(\rho\boldsymbol{V}) = 0, \quad \nabla\times(\boldsymbol{V}\times\boldsymbol{B}) = 0, \tag{2}$$

where $\boldsymbol{B}$, $\boldsymbol{V}$, $-\nabla\mathcal{V}$ are the magnetic, velocity and external gravity fields, respectively, while ρ and P denote the gas density and pressure. With axisymmetry ($\partial/\partial\phi = 0$), we may introduce the magnetic flux function A, such that three free integrals $\Psi(A), \Omega(A), L(A)$ exist (ST94). In terms of these integrals and the square of the poloidal Alfvén number,

$$M^2 = \frac{4\pi\rho V_{\rm p}^2}{B_{\rm p}^2} = \frac{\Psi_A^2}{4\pi\rho}, \tag{3}$$

the magnetic field and bulk flow speed are given in cylindrical coordinates (ϖ, ϕ, z) by the forms

$$\boldsymbol{B} = \frac{\nabla A\times\hat{\boldsymbol{\phi}}}{\varpi} - \frac{L\Psi_A - \varpi^2\Omega\Psi_A}{\varpi(1-M^2)}\hat{\boldsymbol{\phi}},$$

$$\boldsymbol{V} = \frac{\Psi_A}{4\pi\rho}\frac{\nabla A\times\hat{\boldsymbol{\phi}}}{\varpi} + \frac{\varpi^2\Omega - LM^2}{\varpi(1-M^2)}\hat{\boldsymbol{\phi}}, \tag{4}$$

while force balance in the poloidal plane is expressed by the transfield equation (Hu & Low 1989),

$$\frac{(1-M^2)}{4\pi\varpi^2}\left[\varpi\frac{\partial}{\partial\varpi}\left(\frac{1}{\varpi}\frac{\partial A}{\partial\varpi}\right) + \frac{\partial^2 A}{\partial z^2}\right]\nabla A$$
$$- \frac{1}{4\pi\varpi}\frac{\partial M^2(\varpi, A)}{\partial\varpi}\frac{\partial A}{\partial z}\boldsymbol{B}_{\rm p} + +M^2\nabla\left[\frac{(\nabla A)^2}{8\pi\varpi^2}\right] + \nabla P$$
$$+ \rho\nabla\mathcal{V} + \frac{B_\phi}{4\pi\varpi}\nabla(\varpi B_\phi) - \hat{\boldsymbol{\varpi}}\frac{\rho V_\phi^2}{\varpi} = 0. \tag{5}$$

If P is related to ρ and A, for example, via a polytropic relationship with constant or variable polytropic index γ, this last vector equation leads to two scalar equations in any two independent directions on the poloidal plane for the unknowns A and M^2 (or, equivalently, A and ρ). Quasi-analytical solutions of equation (5) have been found only by additionally assuming a self-similar Ansatz for the dependence of the physical variables on the spherical (r, θ) or cylindrical coordinates (ϖ, z) of the poloidal plane. Thus, we have available solutions which are self-similar in (i) the cylindrical radius ϖ (Chan & Henriksen 1980; Bacciotti & Chiuderi 1992), (ii) the spherical radius r (Blandford & Payne 1982; Contopoulos & Lovelace 1994; Fiege & Henriksen 1996) and (iii) the meridional angle θ (Tsinganos & Trussoni 1991; ST94).

In the following we shall consider an infinitely long jet where, in a direction perpendicular to the flow axis, the outwards-directed centrifugal force is balanced by the inwards tension of the toroidal magnetic field and gradient of the magnetic pressure, enhanced (reduced) by the gradient of the gas pressure,

$$\frac{\rho V_\phi^2}{\varpi} = \frac{\rm d}{{\rm d}\varpi}\left[\frac{B_\phi^2}{8\pi} + P\right] + \frac{B_\phi^2}{4\pi\varpi}, \tag{6}$$

where ϖ is the cylindrical distance in spherical coordinates (r, θ, ϕ), $\varpi = r\sin\theta$. In such a case of an asymptotically ($r\to\infty$) collimated outflow (jet) (Heyvaerts & Norman 1989), the magnetic flux function A_∞, Alfvén number M_∞ and gas pressure P_∞ all become functions of the cylindrical distance ϖ at large radial distances r (in comparison with the Alfvén radius $r_\star$) from the source of the outflow where we may neglect the gravitational field,

$$A_\infty = A_\infty(\varpi),\ M_\infty^2 = M_\infty^2(\varpi),\ P_\infty(\varpi) = \int\mathcal{F}_0{\rm d}\varpi, \tag{7}$$

where the pressure gradient $\mathcal{F}_0$ is given in Appendix A. For example, in the cases of cylindrical collimation of ST94 and Contopoulos & Lovelace (1994), $M_\infty(\varpi) =$ constant; while $A_\infty(\varpi)\propto\varpi^2$, or $A_\infty(\varpi)\propto\varpi^F$, for a constant F, in ST94, or Contopoulos & Lovelace (1994), respectively.

In the following we shall investigate the *topological* or structural stability of such collimated solutions. In other words, we are interested in checking whether there exist small-amplitude steady and axisymmetric perturbations in the streamline shape, Alfvén number and pressure, which satisfy equation (5). We are interested in deriving the dependence of these perturbations on the radial distance from the central object. Consider then a solution which is topologically close to one describing a collimated outflow, equation (7),

$$A = A_\infty(\varpi)(1+\varepsilon), \quad M^2 = M_\infty^2(\varpi)\left(1+\varepsilon_1\right),$$
$$P = P_\infty(\varpi) + \delta P, \tag{8}$$

where all functions $|\varepsilon|, |\varepsilon_1|$ and $|\delta P/P_\infty| \ll 1$. By substituting equations (8) into equation (5) and by assuming that the derivatives of $\varepsilon, \varepsilon_1$ are also very small (so that we may ignore squares and products of the perturbation quantities), we obtain from the $\hat{z}$ and

$\hat{\boldsymbol{\varpi}}$ components of the momentum equation (1) two equations which the perturbations ε, ε_1 and δP satisfy

$$\delta P = \mathcal{F}_1\varepsilon + \mathcal{F}_2\varepsilon_1 + \mathcal{F}_3\frac{\partial\varepsilon}{\partial\varpi}, \tag{9}$$

$$\frac{\partial\delta P}{\partial\varpi} = \left(\mathcal{F}_1' + \mathcal{G}_1\mathcal{G}_0\right)\varepsilon + \left(\mathcal{F}_2' + \mathcal{G}_2\mathcal{G}_0\right)\varepsilon_1 + \mathcal{G}_3\frac{\partial\varepsilon}{\partial\varpi} + \mathcal{G}_4\frac{\partial\varepsilon_1}{\partial\varpi} + \mathcal{G}_5\frac{\partial^2\varepsilon}{\partial\varpi^2} + \mathcal{G}_0\frac{\partial^2\varepsilon}{\partial z^2}, \tag{10}$$

or (because of equation 9)

$$\frac{\partial^2\varepsilon}{\partial z^2} + \frac{\partial^2\varepsilon}{\partial\varpi^2} + \left(\frac{2A'}{A} - \frac{1}{\varpi}\right)_\infty\frac{\partial\varepsilon}{\partial\varpi} - \left(\frac{M^2}{1-M^2}\frac{A'}{A}\right)_\infty\frac{\partial\varepsilon_1}{\partial\varpi} + \mathcal{G}_2\varepsilon_1 + \mathcal{G}_1\varepsilon = 0. \tag{11}$$

The perturbations ε, ε_1 and δP satisfy the above equations containing the lengthy general expressions $[\mathcal{F}_1(\varpi), \mathcal{F}_2(\varpi), \mathcal{F}_3(\varpi)]$ and $[\mathcal{G}_0(\varpi), \mathcal{G}_1(\varpi), \mathcal{G}_2(\varpi), \mathcal{G}_3(\varpi), \mathcal{G}_4(\varpi), \mathcal{G}_5(\varpi)]$ which are all given in Appendix A.

The previous analysis is independent of a specific polytropic relationship between pressure and density, and of some particular dependence of the perturbations ε, ε_1 and δP on their variables, as well as of any special choice of the free integrals $\Psi_A(A)$, $L(A)$ and $\Omega(A)$. In order to get some insight into the behaviour of the perturbations, one should analyse the above general non-linear equation. This is, however, a formidable mathematical task, and instead it occurred to us that some physical understanding of the physical trends of the perturbations can be gained by examining separately (a) the case where the perturbations in streamline shape and Alfvén number are related, (b) the case where the perturbations in streamline shape and Alfvén number are unrelated, and (c) the case where a *constant*-index polytropic relation between pressure and density is assumed. In each of the above cases (a), (b) and (c), we shall further examine separately the various cases where a separation of the variables in the perturbations ε and ε_1 is possible. Finally, in each such subcase, we shall apply the results of our analysis to the few examples where special sets of the free integrals $\Psi_A(A)$, $L(A)$ and $\Omega(A)$ have provided known quasi-analytical solutions.

3 LINEARLY RELATED PERTURBATIONS, $\boldsymbol{\varepsilon_1 = \lambda_0(\varpi)\varepsilon}$

In order to make further progress, we shall first examine the case where the perturbations ε and ε_1 are linearly related,

$$\varepsilon_1 = \lambda_0(\varpi)\varepsilon. \tag{12}$$

No specific polytropic relationship between pressure and density is imposed at this stage, where the pressure perturbation is given by equation (9) while ε and $\lambda_0(\varpi)$ satisfy equation (11) which now becomes

$$\frac{\partial^2\varepsilon}{\partial z^2} + \frac{\partial^2\varepsilon}{\partial\varpi^2} + \left[\frac{A'}{A}\left(2 - \frac{\lambda_0 M^2}{1-M^2}\right) - \frac{1}{\varpi}\right]_\infty\frac{\partial\varepsilon}{\partial\varpi} + \left[\mathcal{G}_1 + \lambda_0\mathcal{G}_2 - \lambda_0'\frac{M^2}{1-M^2}\frac{A'}{A}\right]_\infty\varepsilon = 0. \tag{13}$$

The above equation, obtained by substituting equation (12) into equation (11), relates the two unknown functions ε and λ_0 and their derivatives. However, it is still too complicated for a general analysis; in the following, we shall analyse equation (13) in some special cases where the variables of the perturbations can be separated in various coordinates of the poloidal plane.

3.1 Perturbations separable in cylindrical and spherical coordinates

Assume that the variables of the cylindrical and radial distances (ϖ, r) are separable in ε,

$$\varepsilon = f(\varpi)g(r), \qquad |g| \ll 1. \tag{14}$$

Then equation (13) gives

$$g'' + \frac{g'}{r}\left\{2\varpi\frac{f'}{f} + \varpi\frac{A'}{A}\left(2 - \frac{\lambda_0 M^2}{1-M^2}\right)\right\}_\infty + g\left\{\frac{f''}{f} + \left[\frac{A'}{A}\left(2 - \frac{\lambda_0 M^2}{1-M^2}\right) - \frac{1}{\varpi}\right]\frac{f'}{f} + \mathcal{G}_1 + \lambda_0\mathcal{G}_2 - \frac{\lambda_0' M^2}{1-M^2}\frac{A'}{A}\right\}_\infty = 0. \tag{15}$$

Therefore (Appendix B), there are constants (s, k) such that

$$g'' + 2s\frac{g'}{r} + k^2 g = 0, \tag{16}$$

or

$$x^2\frac{\mathrm{d}^2 y}{\mathrm{d}x^2} + x\frac{\mathrm{d}y}{\mathrm{d}x} + \left[x^2 - \left(s - \frac{1}{2}\right)^2\right]y = 0,$$

$$x = kr, \qquad y = gx^{s-\frac{1}{2}}. \tag{17}$$

The last differential equation is the familiar Bessel differential equation with the solution

$$y = D_1 J_{s-\frac{1}{2}}(x) + D_2 Y_{s-\frac{1}{2}}(x). \tag{18}$$

In the limit $x \to \infty$, Bessel's functions become

$$J_\nu(x) \to \frac{1}{\sqrt{x}}\cos\left(x - \frac{\nu\pi}{2} - \frac{\pi}{4}\right),$$

$$Y_\nu(x) \to \frac{1}{\sqrt{x}}\sin\left(x - \frac{\nu\pi}{2} - \frac{\pi}{4}\right), \tag{19}$$

and therefore the solution of (16) is

$$g = \frac{D}{r^s}\sin\left(kr + \phi_0\right). \tag{20}$$

Finally, equation (15) gives two conditions relating the functions of ϖ:

$$\left\{2\varpi\frac{f'}{f} + \varpi\frac{A'}{A}\left(2 - \frac{\lambda_0 M^2}{1-M^2}\right)\right\}_\infty = 2s \tag{21}$$

and

$$\left\{\frac{f''}{f} + \left[\frac{A'}{A}\left(2 - \frac{\lambda_0 M^2}{1-M^2}\right) - \frac{1}{\varpi}\right]\frac{f'}{f} + \mathcal{G}_1 + \lambda_0\mathcal{G}_2 - \frac{\lambda_0' M^2}{1-M^2}\frac{A'}{A}\right\}_\infty = k^2. \tag{22}$$

In the following we shall test our analysis by comparing it with available exact solutions of analytical models of outflows that exhibit an oscillatory behaviour.

3.1.1 *Example 1*

We may start with the simplest case wherein M_∞, λ_0, f, $\mathcal{G}_1$ and $\mathcal{G}_2$ are constants and $A_\infty(\varpi) \propto \varpi^2$. Indeed this case has been studied in ST94 (see also Trussoni et al. 1996). They considered the following expressions of the free integrals:

$$A = \frac{r_\star^2 B_\star}{2}\alpha(R,\theta), \quad \Psi_A(\alpha) = \frac{4\pi\rho_\star V_\star}{B_\star}\sqrt{1+\delta\alpha},$$

$$\alpha = \frac{\varpi^2}{r_\star^2 G^2(R)}, \quad R = \frac{r}{r_\star}, \tag{23}$$

$$L(\alpha) = \lambda r_\star V_\star \frac{\alpha}{\sqrt{1+\delta\alpha}}, \qquad \Omega(\alpha) = \frac{\lambda V_\star}{r_\star}\frac{1}{\sqrt{1+\delta\alpha}}, \tag{24}$$

where $G(R)$ is the radius of the jet in units of the Alfvén radius and λ, δ and $G(R\to\infty) = G_\infty$ are constants, while the starred quantities refer to values at the Alfvén radius $r_\star$. Writing down the expressions of the perturbations for this case we have

$$\varepsilon(r) = \frac{G_\infty^2}{G^2(r)} - 1, \qquad \varepsilon_1(r) = \frac{M^2(r)}{M_\infty^2} - 1\,. \tag{25}$$

It follows from equations (21) and (22) that $f(\varpi) = 1$ while λ_0 is a constant which furthermore can be calculated at $r = r_\star$,

$$\lambda_0 \equiv -|\lambda_0| = -\frac{M_\infty^2 - 1}{M_\infty^2(G_\infty^2 - 1)}\,. \tag{26}$$

This is the same result as that in the study of ST94, although the surface $r = r_\star$ is not always in the asymptotic regime where gravity is negligible. The functions $\mathcal{G}_1$ and $\mathcal{G}_2$ given in Appendix A are constants in this model, and from equations (21) and (22) the corresponding expressions for s and k are

$$s = 2 + \frac{\lambda_0 M_\infty^2}{M_\infty^2 - 1}, \tag{27}$$

$$k^2 \equiv \frac{4\pi^2}{\Lambda_{\rm osc}^2} = \frac{2\lambda^2}{r_\star^2\left(1-M_\infty^2\right)^2}\left[2 - \lambda_0\frac{\left(2M_\infty^2-1\right)G_\infty^4 - M_\infty^4}{M_\infty^2\left(1-M_\infty^2\right)}\right]. \tag{28}$$

The wavelength of the oscillations grows quadratically with the Alfvén number, $\Lambda_{\rm osc} \propto M_\infty^2$, while the amplitude of the oscillations drops with distance as $r^{-(2-|\lambda_0|)}$, as found in ST94 (their figs 2, 8 and 10). For example, as the magnitude of the asymptotic Alfvén number M_∞ increases by a factor of about 10 when the energetic parameter ϵ in the ST94 notation decreases from $\epsilon = 10$ to $\epsilon = 1$, $\Lambda_{\rm osc}$ increases accordingly by a factor of about 100. Similarly, the amplitude of the oscillations $\Lambda_{\rm osc}$ in the width of the jet and the Alfvén number drops with radial distance as r^{-s}, where $1 < s < 2$ with its exact value $s = 2 - |\lambda_0|$ depending on M_∞ and G_∞, according to equation (27).

3.1.2 *Example 2*

Another more general class of solutions can be generated by the following set of free integrals:

$$A = \frac{r_\star^2 B_\star}{2}\alpha(R,\theta),\ \Psi_A(\alpha) = \frac{4\pi\rho_\star V_\star}{B_\star}\sqrt{1+\delta\alpha+\mu\delta_0\alpha^\epsilon},$$

$$\alpha = \frac{\varpi^2}{r_\star^2 G(R)^2}, \quad L(\alpha) = r_\star V_\star \alpha\sqrt{\frac{\xi+\mu\alpha^{\epsilon-1}}{1+\delta\alpha+\mu\delta_0\alpha^\epsilon}},$$

$$\Omega(\alpha) = \frac{V_\star}{r_\star}\sqrt{\frac{\xi+\mu\alpha^{\epsilon-1}}{1+\delta\alpha+\mu\delta_0\alpha^\epsilon}}, \tag{29}$$

where μ, ϵ, δ_0, ξ are constants, in addition to the ones introduced in the previous example. If M_∞, λ_0 and f are constants then

$$k^2 = \frac{2\xi(\epsilon-1)\left(G_\infty^4 - M_\infty^2\right)}{r_\star^2 M_\infty^2\left(1-M_\infty^2\right)^2} \approx \frac{2\xi(1-\epsilon)}{r_\star^2 M_\infty^4} \tag{30}$$

because $M_\infty^2 \gg 1$,

$$\lambda_0 = \left[(\epsilon+1)M_\infty^2 - (\epsilon-1)G_\infty^4\right]\frac{1-M_\infty^2}{\left(2M_\infty^2-1\right)G_\infty^4 - M_\infty^4}, \tag{31}$$

and

$$s = 2 + \frac{\lambda_0 M_\infty^2}{M_\infty^2 - 1} \approx \epsilon + 3\,. \tag{32}$$

Substituting in equation (8) the above expressions for k and s, we find the perturbed form of the streamfunction,

$$A \approx \frac{B_\star \varpi^2}{2G_\infty^2}\left\{1 + \frac{D_0}{R^{\epsilon+3}}\sin\left[\frac{\sqrt{2\xi(1-\epsilon)}}{M_\infty^2}R + \phi_0\right]\right\}. \tag{33}$$

A comparison of the oscillatory behaviour of a solution obtained by this *perturbative* analysis with the corresponding *exact* solution, obtained by integrating the MHD equations and selecting a super-fast solution crossing the (modified by self-similarity) fast critical point, is shown in Figs 1 and 2. In Fig. 1 the dimensionless radial speed oscillates with the dimensionless radial distance, while in Fig. 2 the shape of the streamlines in the poloidal plane shows a similar behaviour. Since by assumption the present perturbation analysis applies to large distances where gravity is negligible and the jet starts approaching its cylindrical shape, such a comparison is meaningful far away from the Alfvén surface, $r \gg r_\star$. Then, the purpose of Figs 1 and 2 is to show by a specific example that at such distances the perturbation analysis gives results which compare rather well with the corresponding exact solution. Also, with the perturbation analysis being independent of any specific model, this comparison shows that the effect of the oscillations is rather model-independent, as discussed in the previous section.

For the specific example shown in Figs 1 and 2, the amplitude of the oscillations in the strength of the radial speed is rather low, at the 3 per cent level; although the same oscillatory behaviour has also been found for other parameters, yielding larger amplitudes of the oscillations close to the 10 per cent level, similarly to the ST94 solution. However, a peculiarity of the present model equation (29) is that the crossing of the critical point becomes numerically rather difficult for parameters giving larger amplitude oscillations. Also, such a crossing of the critical point is the main difficulty in obtaining exact solutions (Tsinganos et al. 1996). Hence, in the illustrations shown in Figs 1 and 2 we have been restricted to a case with an unambiguous crossing of the critical point. In other words, numerical difficulties prohibit the construction of exact solutions with larger amplitudes of oscillation, unlike the case of ST94. Nevertheless, and as discussed in the previous section, the physics of the oscillations remains the same.

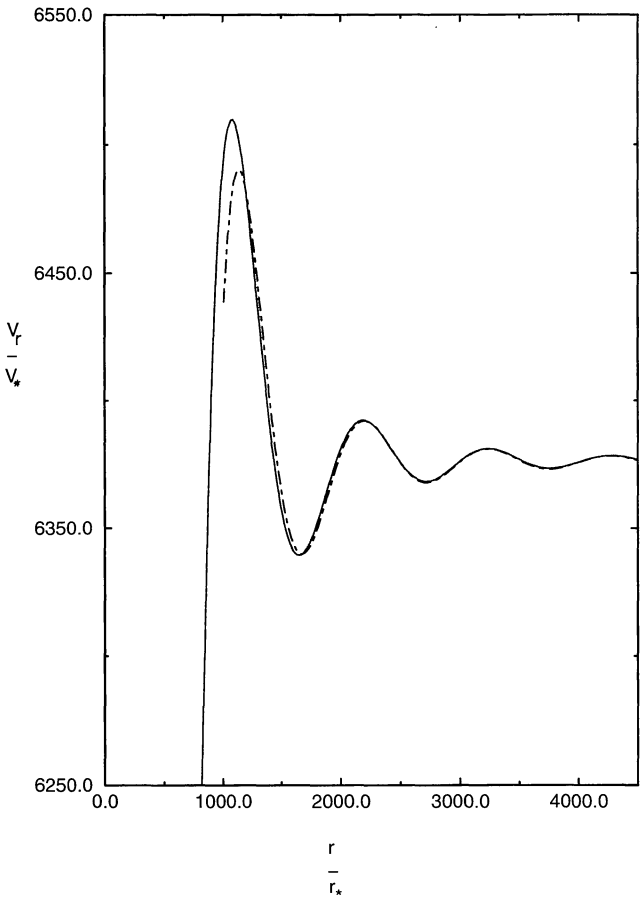

Figure 1. Dimensionless radial velocity V_r on the rotation/magnetic axis versus dimensionless radial distance R. The solid curve indicates the superfast exact solution of the model of example 2 for the following set of parameters: $\epsilon = 0.1$, $\delta = 0.35$, $\delta_0 = 0.01$, $\xi = 5$, $\mu = 0.01$, $2GM/r_\star V_\star^2 = 10$. From the integration of the MHD equation (5) we find that $M_\infty^2 = 490.24$, $G_\infty^2 = 0.0769$. The dashed line indicates the corresponding solution which emerges from the perturbation analysis with $D_0 = 2.79 \times 10^7, \phi_0 = 0.46$.

3.2 Perturbations separable in cylindrical distance and meridional angle

Assume next that the variables of the cylindrical distance and meridional angle (ϖ, θ) are separable in ε,

$$\varepsilon = f(\varpi)g(\theta), \qquad |g| \ll 1. \tag{34}$$

Then equation (13) gives

$$\sin^2\theta g'' + \sin\theta\cos\theta g' \left\{ 2\varpi\frac{f'}{f} + \varpi\frac{A'}{A}\left(2 - \frac{\lambda_0 M^2}{1-M^2}\right) - 1 \right\}_\infty + g\varpi^2 \left\{ \frac{f''}{f} + \left[\frac{A'}{A}\left(2 - \frac{\lambda_0 M^2}{1-M^2}\right) - \frac{1}{\varpi} \right]\frac{f'}{f} + \mathcal{G}_1 + \lambda_0 \mathcal{G}_2 - \frac{\lambda_0' M^2}{1-M^2}\frac{A'}{A} \right\}_\infty = 0. \tag{35}$$

Therefore (Appendix B), there are constants μ, ν with $\mu \geq 0$ such that

$$\sin^2\theta g'' + (2\nu + 1)\sin\theta\cos\theta g' + (\nu^2 - \mu^2)g = 0, \tag{36}$$

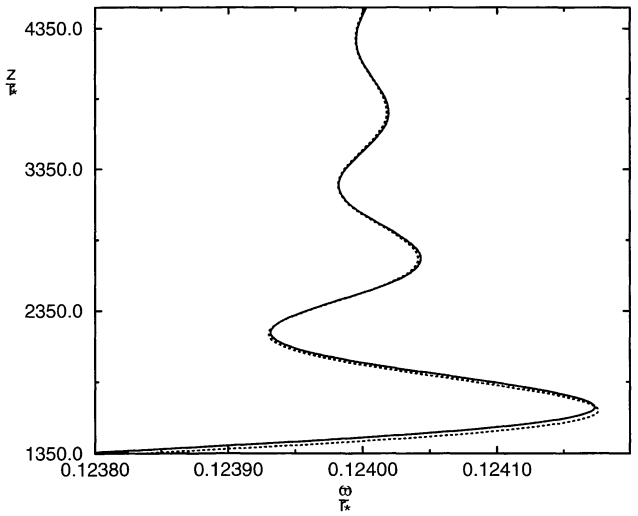

Figure 2. Shape of the streamline on the poloidal plane for the model of example 2, which emerges from the perturbation analysis ($D_0 = 2.79 \times 10^7, \phi_0 = 0.46$). With the dotted line an exact solution is shown for the model of example 2 where gravity is included.

or

$$(1-x^2)\frac{d^2y}{dx^2} - 2x\frac{dy}{dx} + \left[\nu(\nu+1) - \frac{\mu^2}{1-x^2}\right]y = 0, \tag{37}$$

where

$$x = \cos\theta, \qquad y = g\sin^\nu\theta. \tag{38}$$

The last differential equation is the associated Legendre equation, and the solution is given in terms of the associated Legendre functions $P_\nu^\mu(x)$ and $Q_\nu^\mu(x)$ which also show an oscillatory behaviour with the angle $\theta(x)$ that is similar to the Bessel functions of the previous section (Abramowitz & Stegun 1972),

$$y = D_1 P_\nu^\mu(x) + D_2 Q_\nu^\mu(x). \tag{39}$$

Furthermore, equation (35) gives two conditions for the functions of ϖ:

$$\left\{ 2\varpi\frac{f'}{f} + \varpi\frac{A'}{A}\left(2 - \frac{\lambda_0 M^2}{1-M^2}\right) \right\}_\infty = 2\nu + 2 \tag{40}$$

and

$$\left\{ \frac{f''}{f} + \left[\frac{A'}{A}\left(2 - \frac{\lambda_0 M^2}{1-M^2}\right) - \frac{1}{\varpi} \right]\frac{f'}{f} + \mathcal{G}_1 + \lambda_0\mathcal{G}_2 - \frac{\lambda_0' M^2}{1-M^2}\frac{A'}{A} \right\}_\infty = \frac{\nu^2 - \mu^2}{\varpi^2}. \tag{41}$$

It is worth noting that equations (40) and (41) are identical to the corresponding equations (21) and (22) except for the factor ϖ^2 in the denominator of equation (41). The wavelength of the oscillations was found constant in Section 3.1, while now it varies with distance.

3.3 Perturbations separable in cylindrical and axial distances

Assume finally that the variables of the cylindrical and axial distances (ϖ, z) are separable in ε,

$$\varepsilon = f(\varpi)g(z), \qquad |g| \ll 1. \tag{42}$$

Then equation (13) gives

$$g'' + g\left\{\frac{f''}{f} + \left[\frac{A'}{A}\left(2 - \frac{\lambda_0 M^2}{1-M^2}\right) - \frac{1}{\varpi}\right]\frac{f'}{f} + \mathcal{G}_1 + \lambda_0 \mathcal{G}_2 - \frac{\lambda_0' M^2}{1-M^2}\frac{A'}{A}\right\}_\infty = 0. \tag{43}$$

Proceeding as before (Appendix B), it follows that there is constant k such that

$$g'' + k^2 g = 0 \Leftrightarrow g = D\sin(kz + \phi_0), \tag{44}$$

and the oscillations are undamped in this case. This result should be expected because now the radial distance r with its associated scale $r = r_\star$ does not enter directly into the analysis, while with the neglect of gravity the distance z along the jet does not have any associated scale.

4 UNRELATED PERTURBATIONS

Non-oscillating jet-type solutions have been also found recently (Trussoni et al. 1996), and they also emerge from this topological stability analysis by considering the case where the perturbations in the streamline shape and Alfvén number are uncoupled. Assume for simplicity that $\varepsilon = g(r)$ and $\varepsilon_1 = g_1(r)$. For $A_\infty = \lambda_A \varpi^2$, λ_A = constant and $M_\infty^{2'} = 0$, equation (11) takes the form

$$g'' + 4\frac{g'}{r} - \frac{2M_\infty^2}{1-M_\infty^2}\frac{g_1'}{r} + \mathcal{G}_1 g + \mathcal{G}_2 g_1 = 0. \tag{45}$$

Then (Appendix B), there are constants c_1, c_2 such that

$$g'' + 4\frac{g'}{r} - \frac{2M_\infty^2}{1-M_\infty^2}\frac{g_1'}{r} + c_1 g + c_2 g_1 = 0. \tag{46}$$

Comparing this with equation (45) it follows that

$$(\mathcal{G}_1 - c_1)g + (\mathcal{G}_2 - c_2)g_1 = 0. \tag{47}$$

From this last equation two possibilities emerge. The first, where g and g_1 are proportional to each other, has been already studied in Section 3.1, and it was found to give an oscillatory behaviour. The second one corresponds to setting $\mathcal{G}_1 = c_1$ and $\mathcal{G}_2 = c_2$. By solving these equations we find then the following general expressions:

$$\left(\frac{L\Psi_A}{A}\right)_\infty^2 = c_0 \frac{2M_\infty^2 - 1}{\lambda_A^2 M_\infty^4} A_\infty^{-2\frac{2M_\infty^2-1}{M_\infty^2-1}} + \frac{c_1(1-M_\infty^2)^2}{\lambda_A^2}, \tag{48}$$

$$(\Omega\Psi_A)_\infty^2 = c_0 A_\infty^{-2\frac{2M_\infty^2-1}{M_\infty^2-1}} + \frac{M_\infty^2(1-M_\infty^2)^2}{2M_\infty^2-1}\left[c_1 M_\infty^2 - 2c_2\lambda_A^2(1-M_\infty^2)\right], \tag{49}$$

where c_0 is a constant. In other words, if the functions of A $L\Psi_A(A)/A$ and $\Omega\Psi_A(A)$ are given by equations (48) and (49), the corresponding solutions may not exhibit an oscillatory behaviour. So the above conditions are the necessary (but not sufficient) conditions for the appearance of oscillations in the asymptotic regime of collimated outflows, if ε and ε_1 are functions only of r.

4.1 Examples

For the case that has been studied by Trussoni et al. (1996) the free integrals are given by equations (23) and (24) with $\lambda_A = B_\star/2G_\infty^2$. Their non-oscillating solutions there correspond in the notation of the previous section to

$$c_0 = 0, \quad c_2 = -2\lambda^2 \frac{(2M_\infty^2 - 1)G_\infty^4 - M_\infty^4}{r_\star^2 M_\infty^2 (1-M_\infty^2)^3},$$

$$c_1 = \frac{\lambda^2 B_\star^2}{r_\star^2 G_\infty^4 (1-M_\infty^2)^2}. \tag{50}$$

Another general class of solutions can be generated by the set of free integrals given by equations (29). Non-oscillating solutions also exist within this model for the following values of the constants:

$$c_0 = \frac{\lambda^2 B_\star^2}{r_\star^2\left(\frac{B_\star r_\star^2}{2}\right)^{\epsilon-1}}, \quad c_2 = 0, \quad c_1 = \frac{\mu\lambda^2 B_\star^2}{r_\star^2 G_\infty^4 (1-M_\infty^2)^2}, \tag{51}$$

$$M_\infty^2 = \frac{\epsilon+1}{\epsilon+3}, \quad G_\infty^4 = \frac{(\epsilon+1)^2}{(\epsilon-1)(\epsilon+3)}. \tag{52}$$

5 POLYTROPIC MODELS

Assume now that there exists a polytropic relation between density and pressure:

$$P \propto \rho^\gamma \quad \text{or} \quad PM^{2\gamma} = Q(A), \tag{53}$$

for some constant index γ. For a small perturbation this relation becomes

$$(P_\infty + \delta P)M_\infty^{2\gamma}(1+\varepsilon_1)^\gamma = Q_\infty + \delta Q, \tag{54}$$

with

$$Q_\infty(\varpi) = P_\infty M_\infty^{2\gamma}, \tag{55}$$

and

$$\delta Q = \left(\frac{\mathrm{d}Q}{\mathrm{d}A}\right)_\infty A_\infty \varepsilon = \frac{Q_\infty' A_\infty}{A_\infty' Q_\infty}\varepsilon. \tag{56}$$

Substituting the pressure perturbation from equations (54)–(56) in equation (9) gives

$$(\mathcal{F}_2 + \gamma P_\infty)\varepsilon_1 = \left[\frac{A}{A'}\left(\mathcal{F}_0 + \gamma\frac{P_\infty M^{2'}}{M^2}\right) - \mathcal{F}_1\right]_\infty \varepsilon - \mathcal{F}_3\frac{\partial\varepsilon}{\partial\varpi}. \tag{57}$$

We shall distinguish two cases:

(a) $\mathcal{F}_2 + \gamma P_\infty = 0$,

$$\mathcal{F}_3\frac{\partial\varepsilon}{\partial\varpi} = \left[\frac{A}{A'}\left(\mathcal{F}_0 + \gamma\frac{P_\infty M^{2'}}{M^2}\right) - \mathcal{F}_1\right]_\infty \varepsilon, \tag{58}$$

and

(b) $\mathcal{F}_2 + \gamma P_\infty \neq 0$, $\quad \varepsilon_1 = \mathcal{K}_1\varepsilon + \mathcal{K}_2\frac{\partial\varepsilon}{\partial\varpi}$. (59)

In case (a), we may solve equation (58) and obtain, for each of the particular dependences of ε, the following three cases:

(i) for $\varepsilon = f(\varpi)g(r)$,

$$\varepsilon = \exp\left[-\left(\frac{r}{r_0}\right)^2\right] \times \exp\left[\left(\frac{\varpi}{r_0}\right)^2\right] \exp\left\{\int \frac{\left[\frac{A}{A'}\left(\mathcal{F}_0 + \gamma\frac{P_\infty M^{2'}}{M^2}\right) - \mathcal{F}_1\right]_\infty}{\mathcal{F}_3}\mathrm{d}\varpi\right\}; \tag{60}$$

(ii) for $\varepsilon = f(\varpi)g(\theta)$,

$$\varepsilon = (\tan\theta)^{\lambda}\varpi^{-\lambda}\exp\left\{\int\frac{\left[\frac{A}{A'}\left(\mathcal{F}_0+\gamma\frac{P_\infty M^{2'}}{M^2}\right)-\mathcal{F}_1\right]_\infty}{\mathcal{F}_3}\mathrm{d}\varpi\right\}; \quad (61)$$

(iii) for $\varepsilon = f(\varpi)g(z)$,

$$\varepsilon = g(z)\exp\left\{\int\frac{\left[\frac{A}{A'}\left(\mathcal{F}_0+\gamma\frac{P_\infty M^{2'}}{M^2}\right)-\mathcal{F}_1\right]_\infty}{\mathcal{F}_3}\mathrm{d}\varpi\right\}, \quad (62)$$

where g is an arbitrary function of z. In all cases equation (11) gives ε_1.

Case (b) with $\mathcal{F}_2+\gamma P_\infty \neq 0$, on the other hand, turns out to be the most interesting and will be analysed in more detail in the following. Then equation (11) takes the form

$$\mathcal{H}_1\varepsilon+\mathcal{H}_2\frac{\partial\varepsilon}{\partial\varpi}+\mathcal{H}_3\frac{\partial^2\varepsilon}{\partial\varpi^2}+\frac{\partial^2\varepsilon}{\partial z^2}=0. \quad (63)$$

5.1 Perturbations separable in cylindrical and axial distances

Assume first that the variables of the cylindrical and axial distances (ϖ, z) are separable in ε, $\varepsilon = f(\varpi)g(r), |g| \ll 1$. Then equation (63) gives

$$g''\left[1+\frac{\varpi^2(\mathcal{H}_3-1)}{r^2}\right]+\frac{g'}{r}\left[\varpi\mathcal{H}_2+\mathcal{H}_3+2\varpi\mathcal{H}_3\frac{f'}{f}-\frac{\varpi^2(\mathcal{H}_3-1)}{r^2}\right]+g\left(\mathcal{H}_1+\mathcal{H}_2\frac{f'}{f}+\mathcal{H}_3\frac{f''}{f}\right)=0. \quad (64)$$

Therefore (Appendix B), there are constants (s, k, s_1, s_2) such that

$$g''\left(1+\frac{s_1}{r^2}\right)+\frac{g'}{r}\left(2s+\frac{s_2}{r^2}\right)+k^2g=0. \quad (65)$$

The asymptotic solution of the previous equation is the solution of Section 3.1, although the relations between the functions of ϖ are different.

5.2 Perturbations separable in cylindrical distance and meridional angle

Assume next that the variables of the cylindrical distance and meridional angle (ϖ, θ) are separable in ε, $\varepsilon = f(\varpi)g(\theta), |g| \ll 1$. Then equation (63) gives

$$\sin^2\theta g'' + \sin^2\theta\cos^2\theta g''(\mathcal{H}_3-1)+\sin\theta\cos\theta g'\varpi\left(\mathcal{H}_2+2\frac{f'}{f}\mathcal{H}_3\right)-2\sin^3\theta\cos\theta g'\times(\mathcal{H}_3-1)+g\varpi^2\left(\mathcal{H}_1+\mathcal{H}_2\frac{f'}{f}+\mathcal{H}_3\frac{f''}{f}\right)=0. \quad (66)$$

Therefore (Appendix B), there are constants s_1, s_2, s_3, s_4 such that

$$\sin^2\theta g''(1+s_1-s_1\sin^2\theta)+\sin\theta\cos\theta g'(s_3+s_2\sin^2\theta)+s_4g=0. \quad (67)$$

For $s_1=-1$ the solution goes asymptotically as $g=(\tan\theta)^{-s_4/s_3}$, while for the most interesting case of $s_1\neq -1$ we may introduce the new constants μ, ν with $\mu \geq 0$ and $2\nu+1=s_3/(s_1+1)$, $\nu^2-\mu^2=s_4/(s_1+1)$, such that the differential equation for g becomes

$$\sin^2\theta g''\left(1-\frac{s_1}{s_1+1}\sin^2\theta\right)+\sin\theta\cos\theta g'\times\left(2\nu+1+\frac{s_3}{s_1+1}\sin^2\theta\right)+(\nu^2-\mu^2)g=0. \quad (68)$$

The asymptotic solution of the previous equation is similar to the solution of equation (36), i.e. it is given by equation (39), with of course different relations between the functions of ϖ. Oscillations like those predicted by the analysis of this section have indeed been found in the model of Contopoulos & Lovelace (1994), where

$$A\propto\left[\frac{\varpi}{G(\theta)}\right]^F, \qquad \Psi_A\propto A^{1-\frac{3}{2F}},$$
$$L\propto A^{\frac{1}{2F}}, \qquad \Omega\propto A^{-\frac{3}{2F}}, \quad (69)$$

and where (M_∞, λ_0, f) are constants.

5.3 Perturbations separable in cylindrical and axial distances

Finally, assume that the variables of the cylindrical and axial distances (ϖ, z) are separable in ε, $\varepsilon = f(\varpi)g(z), |g| \ll 1$. Then equation (63) gives

$$g''+g\left(\mathcal{H}_1+\mathcal{H}_2\frac{f'}{f}+\mathcal{H}_3\frac{f''}{f}\right)=0. \quad (70)$$

Therefore (Appendix B), there is a constant k such that

$$g''+k^2g=0 \Leftrightarrow g=D\sin(kz+\phi_0), \quad (71)$$

and the oscillations do not decay due to the lack of scale in the direction z, similarly to the case of Section 3.3. Examples of models with such oscillations have been analysed by Chan & Henriksen (1980) and Bacciotti & Chiuderi (1992).

6 DISCUSSION

Previous studies have shown that under fairly general conditions, magnetized outflows may become asymptotically cylindrical (Heyvaerts & Norman 1989). Also, this tendency for asymptotic collimation has been demonstrated via quasi-analytic self-similar solutions (ST94; Contopoulos & Lovelace 1994; Trussoni et al. 1996). A common feature in all such self-similar solutions is that, before the final cylindrical collimation is achieved, the jet passes through a stage of oscillations in its radius, Alfvén number and other physical parameters. In the previous sections we have shown under rather general assumptions that this oscillatory behaviour of collimated outflows is not restricted to the few specific models studied so far, but instead is a rather generic physical property of the MHD outflow as it reaches collimation.

A simple way to demonstrate this effect physically can be provided by the simplified construction shown in Fig. 3. A single streamline $A(\varpi, z)$ = constant of an initially *radial* magnetized and rotating outflow becomes asymptotically *cylindrical* (dashed line). Assume for simplicity that the jet carries an electric current $I_z \propto \varpi^2$ with a uniform surface density J_z = constant. In its asymptotic regime the jet is confined by the interplay of the magnetic pinching force, the gas pressure gradient and the centrifugal force of rotation (ST94; Trussoni et al. 1996). Assume for simplicity that the gas pressure gradient is negligible such that at equilibrium the magnetic

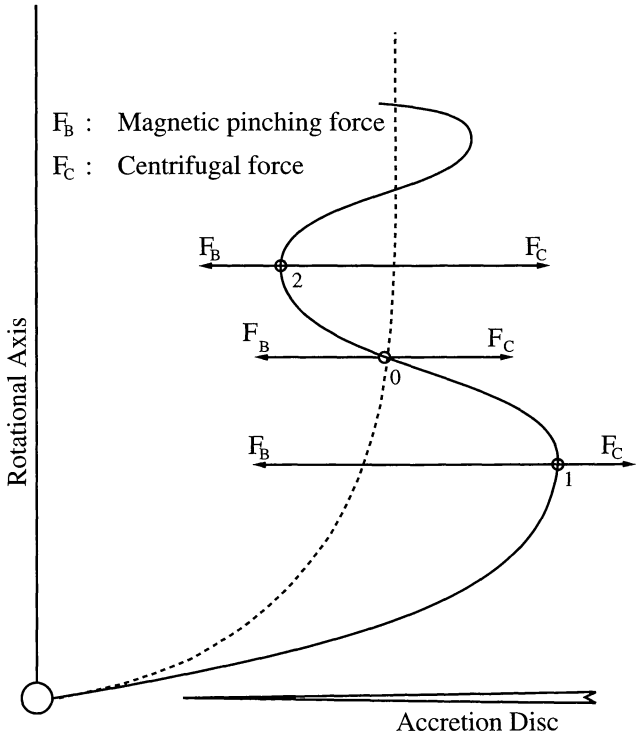

Figure 3. Sketch of an oscillating streamline on the poloidal plane (ϖ, z) of an MHD outflow from a central object. The inwards magnetic pinching force F_B equals the outwards inertial centrifugal force F_C at position 0. At position 1 F_B is greater than F_C while at position 2 F_B is greater than F_C.

pinching force exactly balances the centrifugal force. In the superAlfvénic regime, most of the conserved specific angular momentum is carried by the fluid, such that $L \approx \varpi V_\varphi$. The magnetic pinching force F_B which results from such a current I_z and the centrifugal force F_C for the assumed angular momentum conservation are then

$$F_B = \frac{B_\varphi^2}{4\pi\varpi} + \frac{\partial}{\partial\varpi}\frac{B_\varphi^2}{8\pi} \propto \varpi, \qquad F_C = \frac{\rho V_\varphi^2}{\varpi} \propto \frac{L^2}{\varpi^3}, \tag{72}$$

under uniform density conditions. If now at some equilibrium location 0, say at the cylindrical distance $\varpi = \varpi_0$ on the dashed line in Fig. 3, we have $F_B(\varpi_0) = F_C(\varpi_0)$, then at larger distances $\varpi_1 > \varpi_0$ (location 1 in Fig. 3) we have, according to equation (72), that $F_B(\varpi_1) > F_C(\varpi_1)$. Conversely, at the smaller cylindrical distances $\varpi_2 < \varpi_0$ (location 2 in Fig. 3) we have, again according to equation (72), $F_C(\varpi_2) > F_B(\varpi_2)$. The net result is that as the parcel of gas moves along the poloidal streamline from the central object to infinity, it feels an inward force at location 1 which brings it towards the rotation axis. On the other hand, due to inertia and its poloidal speed, it overshoots the equilibrium position 0 and arrives at location 2 where it now feels an outward force bringing it again away from the rotation axis towards location 0, etc. The final result is the oscillatory shape of the streamline shown in Fig. 3 and derived in the previous sections. The oscillations start at the collimation distance R_c where the streamlines start to deviate significantly from a radial form, and by means of the magnetic pinching forces are brought to the cylindrical geometry. Obviously, at large distances from the collimation radius R_c the cause of the oscillations disappears, and accordingly their amplitude decays to zero, i.e. the uniform cylindrical shape is finally reached. An example of this situation has been given in Trussoni et al. (1996), where $A = f(R)\sin^2\theta$ with $f(R) \approx 1$ at $R \leq R_c$, while further away at $R \geq R_c$, $f(R) \approx R^2$. The poloidal magnetic field of such a case is a typical radial field $B_p \approx B_r = B_*/R^2 \cos\theta$ at $R \leq R_c$, while further away the poloidal magnetic field and flow become rather uniform, similarly to the density at a given streamline.

At the asymptotic and collimated regime of the outflow, we expect that gravity should be negligible. For this reason and in order to simplify the mathematics, in the analysis presented in this paper gravity was not included. Indeed, this assumption is verified by the plot of Figs 1 and 2, where the solid and dotted lines, respectively, give a full solution of the problem by including gravity, while the other lines show the approximate solution which is calculated by neglecting gravity. These two curves almost coincide, with some deviation starting as we approach the source of the flow where gravity becomes rather important.

In the example shown for illustrative purposes in Figs 1 and 2, the oscillations in the magnitudes of the flow speed, temperature, density and pressure of the beam are rather weak at the few per cent level. However, this is only due to the fact that the availability of exact superfast solutions for model 2 is constrained by numerical problems associated with the crossing of the fast critical point. In ST94, stronger oscillations of similar origin at the 10 per cent level have been presented, which also emerge from the present perturbation analysis. Then such large-amplitude oscillations in the initial part of the beam may have notable effects, for example via enhanced radiation emission either in local compressions of the flow pattern or in shock transitions. For example, observed brightness enhancements (knots) along the well-studied jet of M87 in Virgo have been attributed to shocks (Biretta 1996), with a similar situation for stellar jets (Ray 1996). Such shocks may be caused by an oscillatory flow channel, in which case the hydrodynamic equations allow multiple transonic solutions connected by shocks (Ferrari et al. 1986). In the present study we have shown that oscillations in the cross-section of the jet may be due, in addition to the familiar Kelvin–Helmholtz instabilities, to the interplay of the magnetic and inertial forces in the acceleration region of the outflow. Although an examination of the detailed solution topologies of the present MHD case is far more complicated than the corresponding hydrodynamic solution topologies, it is naturally expected that similar shocks connecting various transonic solutions may exist in the present MHD case as well. However, their existence in self-similar MHD solutions is beyond the scope of this paper, and remains a challenge for future studies. It will also be interesting to check whether fully numerical studies of collimated MHD outflows show an oscillatory behaviour in the shape of the streamlines. In the only available such study so far, of a paraboloidally collimated disc wind (Sakurai 1987), such oscillations are not evident.

ACKNOWLEDGMENTS

This research has been supported in part by a grant from the General Secretariat of Research and Technology of Greece. We thank J. Contopoulos, C. Sauty, E. Trussoni and G. Surlantzis for helpful discussions.

REFERENCES

Abramowitz M., Stegun I. A., 1972, Handbook of Mathematical Functions. Dover Publications, Inc., New York
Appl S., 1996, A&A, 314, 995
Appl S., Camenzind M., 1992, A&A, 256, 354
Bacciotti F., Chiuderi C., 1992, Phys. Fluids, 4(1), 35

Biretta T., 1996, in Tsinganos K., ed., Solar and Astrophysical MHD Flows. Kluwer, Dordrecht, p. 357
Blandford R. D., Payne D. G., 1982, MNRAS, 199, 883
Bodo G., Massaglia S., Ferrari A., Trussoni E., 1994, A&A, 283, 655
Bodo G., Massaglia S., Rossi P., Rosner R., Malagoli A., Ferrari A., 1995, A&A, 303, 281
Chan K. L., Henriksen R. N., 1980, ApJ, 241, 534
Contopoulos J., Lovelace R. V. E., 1994, ApJ, 429, 139
Ferrari A., Trussoni E., Zaninetti L., 1978, A&A, 64, 43
Ferrari A., Trussoni E., Zaninetti L., 1981, MNRAS, 196, 1051
Ferrari A., Trussoni E., Rosner R., Tsinganos K., 1986, ApJ, 300, 577
Ferrari A., Massaglia S., Bodo G., Rossi P., 1996, in Tsinganos K., ed., Solar and Astrophysical MHD Flows. Kluwer, Dordrecht, p. 607
Fiege J. D., Henriksen R. N., 1996, MNRAS, 281, 1038
Heyvaerts J., Norman C. A., 1989, ApJ, 347, 1055
Hu Y. Q., Low B. C., 1989, ApJ, 342, 1049
Ray T. P., 1996, in Tsinganos K., ed., Solar and Astrophysical MHD Flows. Kluwer, Dordrecht, p. 539
Sakurai T., 1987, PASJ, 39, 821
Sauty C., Tsinganos K., 1994, A&A, 287, 893 (ST94)
Trussoni E., Sauty C., Tsinganos K., 1996, in Tsinganos K., ed., Solar and Astrophysical MHD Flows. Kluwer, Dordrecht, p. 383
Tsinganos K., Trussoni E., 1991, A&A, 249, 156
Tsinganos K., Sauty C., Surlantzis G., Trussoni E., Contopoulos J., 1996, in Tsinganos K., ed., Solar and Astrophysical MHD Flows. Kluwer, Dordrecht, p. 247

APPENDIX A

$$\mathcal{F}_0(\varpi)=\frac{1}{4\pi\varpi^2}\left[A'\left(\frac{A'}{\varpi}-A''\right)-A'\frac{\frac{\partial}{\partial A}\left(L\Psi_A-\varpi^2\Omega\Psi_A\right)^2}{2\left(1-M^2\right)^2}\right.$$
$$\left.-M^{2'}\frac{\left(L\Psi_A-\varpi^2\Omega\Psi_A\right)^2}{\left(1-M^2\right)^3}\right.$$
$$\left.-\frac{\left(2M^2-1\right)\left(\varpi^2\Omega\Psi_A\right)^2-\left(L\Psi_A\right)^2M^4}{\varpi M^2\left(1-M^2\right)^2}\right]_\infty, \tag{A1}$$

$$\mathcal{F}_1(\varpi)=-\frac{1}{4\pi\varpi^2}\left[\left(1-M^2\right)A\left(A''-\frac{A'}{\varpi}\right)+M^2A'^2\right.$$
$$\left.-M^{2'}AA'+A\frac{\frac{\partial}{\partial A}\left(L\Psi_A-\varpi^2\Omega\Psi_A\right)^2}{2\left(1-M^2\right)^2}\right]_\infty, \tag{A2}$$

$$\mathcal{F}_2(\varpi)=-\frac{1}{4\pi\varpi^2}\left(M^2A'^2+M^2\frac{\left(L\Psi_A-\varpi^2\Omega\Psi_A\right)^2}{\left(1-M^2\right)^3}\right)_\infty, \tag{A3}$$

$$\mathcal{F}_3(\varpi)=-\frac{1}{4\pi\varpi^2}\left(M^2AA'\right)_\infty, \tag{A4}$$

$$\mathcal{G}_0(\varpi)=-\frac{1}{4\pi\varpi^2}\left[AA'\left(1-M^2\right)\right]_\infty, \tag{A5}$$

$$\mathcal{G}_1(\varpi)=\left[\frac{M^2\frac{\mathrm{d}}{\mathrm{d}A}\left(L\Psi_A\right)^2-\varpi^4\frac{\mathrm{d}}{\mathrm{d}A}\left(\Omega\Psi_A\right)^2}{\varpi M^2\left(1-M^2\right)^2A'}\right.$$
$$-\frac{A'''}{A'}+\frac{3A''}{\varpi A'}+\frac{A''}{A}-\frac{A'}{\varpi A}-\frac{3}{\varpi^2}$$
$$\left.+\frac{M^{2''}}{1-M^2}+\frac{M^{2'}}{1-M^2}\left(\frac{2A''}{A'}-\frac{3}{\varpi}\right)\right]_\infty, \tag{A6}$$

$$\mathcal{G}_2(\varpi)=\left[\frac{2M^2}{1-M^2}\left(\frac{A'}{\varpi A}-\frac{A''}{A}\right)-\frac{M^{2'}A'}{A\left(1-M^2\right)}\right.$$
$$\left.+\frac{M^4\left(L\Psi_A\right)^2-\left(2M^2-1\right)\left(\varpi^2\Omega\Psi_A\right)^2}{\varpi M^2\left(1-M^2\right)^3AA'}\right]_\infty, \tag{A7}$$

$$\mathcal{G}_3(\varpi)=-\frac{1}{4\pi\varpi^2}\left[2A'^2-2A\frac{A'}{\varpi}+AA''\right.$$
$$\left.+A\frac{\frac{\partial}{\partial A}\left(L\Psi_A-\varpi^2\Omega\Psi_A\right)^2}{2\left(1-M^2\right)^2}\right]_\infty, \tag{A8}$$

$$\mathcal{G}_4(\varpi)=-\frac{1}{4\pi\varpi^2}\left[M^2\frac{\left(L\Psi_A-\varpi^2\Omega\Psi_A\right)^2}{\left(1-M^2\right)^3}\right]_\infty, \tag{A9}$$

$$\mathcal{G}_5(\varpi)=-\frac{1}{4\pi\varpi^2}\left(AA'\right)_\infty, \tag{A10}$$

$$\mathcal{K}_1(\varpi)=\frac{\left[\frac{A}{A'}\left(\mathcal{F}_0+\gamma\frac{P_\infty M^{2'}}{M^2}\right)-\mathcal{F}_1\right]_\infty}{\mathcal{F}_2+\gamma P_\infty}, \tag{A11}$$

$$\mathcal{K}_2(\varpi)=-\frac{\mathcal{F}_3}{\mathcal{F}_2+\gamma P_\infty}, \tag{A12}$$

$$\mathcal{H}_1(\varpi)=\mathcal{G}_1+\mathcal{K}_1\mathcal{G}_2-\mathcal{K}_1'\left(\frac{M^2}{1-M^2}\frac{A'}{A}\right)_\infty, \tag{A13}$$

$$\mathcal{H}_2(\varpi)=2\left(\frac{A'}{A}\right)_\infty-\frac{1}{\varpi}-\left(\mathcal{K}_1+\mathcal{K}_2'\right)\left(\frac{M^2}{1-M^2}\frac{A'}{A}\right)_\infty+\mathcal{K}_2\mathcal{G}_2, \tag{A14}$$

$$\mathcal{H}_3(\varpi)=1-\mathcal{K}_2\left(\frac{M^2}{1-M^2}\frac{A'}{A}\right)_\infty. \tag{A15}$$

APPENDIX B

Theorem

If $F(x)$, $f_i(x)$, $g_i(y)$, $i=1,2,\ldots,n$, are arbitrary functions of the independent variables x and y and

$$F(x)=f_1(x)g_1(y)+f_2(x)g_2(y)+\cdots+f_n(x)g_n(y), \tag{B1}$$

then there exist constants $c_1,c_2,\ldots,c_n$ such that

$$F(x)=c_1f_1(x)+c_2f_2(x)+\cdots+c_nf_n(x). \tag{B2}$$

Proof

We shall use the method of mathematical induction.

(i) For $n=1$, $F(x)=f_1(x)g_1(y)$.
If $f_1(x)=0$ then $F(x)=0=c_1f_1(x)$.
If $f_1(x)\neq 0$ then

$$\frac{F(x)}{f_1(x)}=g_1(y)=c_1 \quad\Rightarrow\quad F(x)=c_1f_1(x), \tag{B3}$$

i.e. for $n=1$ equation (2) holds.

(ii) Assume that for $n=k$ equation (2) holds, i.e. for given

$$F(x)=f_1(x)g_1(y)+f_2(x)g_2(y)+\cdots+f_k(x)g_k(y) \tag{B4}$$

$\Rightarrow\exists\ c_1,c_2,\ldots,c_k$ such that $F(x)=c_1f_1(x)+c_2f_2(x)+\cdots+c_kf_k(x)$ for every $F,f_i,g_i,i=1,2,\ldots,k$.

(iii) Then, for $n = k+1$, let $F(x) = f_1(x)g_1(y) + \cdots + f_{k+1}(x)g_{k+1}(y)$. If $f_{k+1}(x) = 0$ then from the previous hypothesis

$$F(x) = c_1 f_1(x) + \cdots + c_k f_k(x) = c_1 f_1(x) + \cdots + c_{k+1} f_{k+1}(x), \tag{B5}$$

i.e. equation (2) holds. If, on the other hand, $f_{k+1}(x) \neq 0$ then

$$\frac{F(x)}{f_{k+1}(x)} = \frac{f_1(x)}{f_{k+1}(x)} g_1(y) + \cdots + \frac{f_k(x)}{f_{k+1}(x)} g_k(y) + g_{k+1}(y) \;\Rightarrow \tag{B6}$$

$$\frac{\mathrm{d}}{\mathrm{d}x}\left(\frac{F(x)}{f_{k+1}(x)}\right) = \frac{\mathrm{d}}{\mathrm{d}x}\left(\frac{f_1(x)}{f_{k+1}(x)}\right) g_1(y) + \cdots + \frac{\mathrm{d}}{\mathrm{d}x}\left(\frac{f_k(x)}{f_{k+1}(x)}\right) g_k(y). \tag{B7}$$

So from the hypothesis that for $n = k$ there are c_i such that

$$\frac{\mathrm{d}}{\mathrm{d}x}\left(\frac{F(x)}{f_{k+1}(x)}\right) = c_1 \frac{\mathrm{d}}{\mathrm{d}x}\left(\frac{f_1(x)}{f_{k+1}(x)}\right) + \cdots + c_k \frac{\mathrm{d}}{\mathrm{d}x}\left(\frac{f_k(x)}{f_{k+1}(x)}\right) \Rightarrow \tag{B8}$$

$$\frac{F(x)}{f_{k+1}(x)} = c_1 \frac{f_1(x)}{f_{k+1}(x)} + \cdots + c_k \frac{f_k(x)}{f_{k+1}(x)} + c_{k+1}$$

$$\Leftrightarrow \quad F(x) = c_1 f_1(x) + \cdots + c_{k+1} f_{k+1}(x), \tag{B9}$$

and therefore equation (2) holds for every n.

This paper has been typeset from a TEX/LATEX file prepared by the author.